ELSEVIER

May 1994

Pattern Recognition Letters

Pattern Recognition Letters 15 (1994) 485–496

Edge localization by MoG filters: Multiple-of-Gaussians

Lucas J. van Vliet, Piet W. Verbeek

Pattern Recognition Group, Faculty of Applied Physics, Delft University of Technology, Lorentzweg 1, 2628 CJ Delft, Netherlands

Received 8 July 1993; revised 28 September 1993

Abstract

Zero-crossings in a second-derivative-of-Gaussian filtered image is a well-known edge location criterion. Examples are the Laplacian and directional second derivatives such as the second derivative in the gradient direction (SDGD). Derivative operators can easily be implemented as a convolution with a derivative of a Gaussian.

Gaussian filtering displaces the half height isophote towards smaller edge radii (inwards for convex edges and outwards for concave edges). The Difference-of-Gaussians (DoG) filters are similar to the Laplacian-of-Gaussian and exert an edge shift to larger edge radii (outwards). This paper introduces Multiple-of-Gaussians filters with reduced curvature-based error. Using N Gaussians ($N>2$) we reduce edge shifts to a fraction $(1/(2N-3))$ of the ones produced by a similar Laplacian-of-Gaussian filter.

Key words: Gaussian filter; Laplacian-of-Gaussian; Multi-dimensional edge detection; Edge accuracy

1. Introduction

In our research we have studied the location error of curved edges in 2D and 3D images after analog and digital low-pass filtering. Analog low-pass filtering is unavoidable since the finite aperture of lenses ensures bandlimitation of the imaged object. Digital low-pass filtering is often applied to suppress noise. This paper deals with the systematic displacement of curved edges due to filtering with a linear combination of Gaussians.

In this paper we start with a brief introduction of Multiple-of-Gaussians (MoG) filters and present a brief description of Gaussian filters as a general purpose tool in modeling the image analysis process. Section 3 derives the weight-factors for a linear combination of N Gaussians. The weight-factors are independent of the amount of pre-smoothing and the edge curvature. Section 4 deals with the actual choice of the Gaussian widths $\{\sigma_i\}$. In Section 5 we predict the location error for Gaussian smoothed curved edges. The experiments in Section 6 test the presented theory on simulated test images.

2. Gaussian filters

A normalized multi-dimensional isotropic Gaussian filter of size σ as a function of radius r is given by

* Corresponding author. Email: lucas@ph.tn.tudelft.nl.

SSDI 0167-8655(93)E0095-6

$$G_D(r,\sigma) = (2\pi\sigma^2)^{-D/2}\, e^{-r^2/2\sigma^2} \tag{1}$$

where D is the dimension; usually D is 2 or 3. Note that normalization implies

$$\int\int \ldots \int G_D(r,\sigma)\, dx_1\, dx_2 \ldots dx_D = \int_0^\infty G_D(r,\sigma)\, V(D)\, dr^D = 1 \tag{2}$$

where $x_1^2+x_2^2+\ldots=r^2$ and $V(D)$ is the volume of a D-dimensional hyper-sphere of radius 1

$$V(D) = \pi^{D/2}/\Gamma(\tfrac{1}{2}D+1) \tag{3}$$

with $\Gamma(\cdot)$ the Gamma function. For the first three dimensions ($D=1, 2, 3$) the volume is $V(1)=2$, $V(2)=\pi$, $V(3)=\frac{4}{3}\pi$, respectively. A normalized filter leaves a constant-valued image unchanged. In the remainder of this paper we omit the prefix hyper to spheres (or properties of it such as area and volume) in D-dimensional space.

We choose Gaussian filtering as a general purpose tool in modeling the various stages of the image analysis process. First we model the smooth grey slopes of biological objects as Gaussian-smoothed curved step edges (σ_{slope}), then we approximate the point spread function (PSF) of a microscope by a Gaussian filter (σ_{PSF}). Next we apply a Gaussian filter for noise suppression (Canny, 1986; van Vliet et al., 1989) or scaling (Witkin, 1983; Koenderink, 1984) (σ_{smooth}). These successive filtering steps combine into one still normalized Gaussian filter $G_D(r,\sigma_0)$ with

$$\sigma_0^2 = \sigma_{\text{slope}}^2 + \sigma_{\text{PSF}}^2 + \sigma_{\text{smooth}}^2 .$$

For edge location as the next step in image analysis we propose a linear combination of Gaussian filters (Multiple-of-Gaussians, MoG) that will act as a pseudo second-derivative filter

$$\text{MoG}(r,\{w_i\},\{\sigma_i\},N) \equiv \sum_{i=1}^{N} w_i G_D(r,\sigma_i) \tag{4}$$

with w_i being the weight coefficient for the Gaussian of width σ_i. The combined effect of the filters $G_D(r,\sigma_0)$ and MoG is again a MoG filter

$$\text{MoG}(r,\{w_i\},\{\sigma_i'\},N) \equiv \sum_{i=1}^{N} w_i G_D(r,\sigma_i')$$

with

$$\sigma_i'^2 = \sigma_0^2 + \sigma_i^2 \tag{5}$$

and $1 \leqslant i \leqslant N$. We shall study the position of the central zero-crossing of a curved step edge after MoG filtering.

3. Weights of Gaussians

Before specifying the requirements that the MoG filter has to fulfill to act as a pseudo second-derivative filter, we will calculate the filter response in various situations:

- MoG filter inside an object;
- MoG filter on a straight step edge;
- MoG filter on a constant-curvature step edge.

The response will be expressed in the weights $\{w_i\}$ and the widths $\{\sigma_i'\}$ of the N normalized Gaussians.

3.1. Filter response inside an object

For an arbitrarily shaped object of height 1 in D-dimensional space, using Eq. (2) the MoG filter response inside the object is

$$\int\int \dots \int \mathrm{MoG}(r, \{w_i\}, \{\sigma_i'\}, N)\, \mathrm{d}x_1\, \mathrm{d}x_2 \dots \mathrm{d}x_D = \int_0^\infty \left(\sum_{i=1}^N w_i G_D(r, \sigma_i') \right) V(D)\, \mathrm{d}r^D = \sum_{i=1}^N w_i\,, \tag{6}$$

the sum of the weight coefficients $\{w_i\}$.

3.2. Filter response on a straight step edge

Given a zero-curvature step edge in D-dimensional space (a straight line in 2D, a plane in 3D, etc.), the MoG filter response, when the filter is centered on the edge, is exactly half of the filter response fully inside the object as given in Eq. (6). Thus the MoG filter response when the filter is centered exactly on-edge is

$$\tfrac{1}{2} \int\int \dots \int MoG(r, \{w_i\}, \{\sigma_i'\}, N)\, \mathrm{d}x_1\, \mathrm{d}x_2 \dots \mathrm{d}x_D = \tfrac{1}{2} \sum_{i=1}^N w_i\,. \tag{7}$$

3.3. Filter response on a constant-curvature step edge

For a curved edge the response on the edge is more (concave object) or less (convex object) than $\frac{1}{2}\sum w_i$ as the edge cuts out more or less than half of the filter. The hatched area in Fig. 1 shows the difference in filter response between a straight step edge and a constant-curvature step edge.

Lemma 1. *In the approximation of small edge curvature $\kappa \equiv 1/R$ the MoG filter response of Eq. (7) must be corrected by*

$$\int_0^\infty \left(\sum_{i=1}^N w_i G_D(r, \sigma_i') \right) S\left(D, \frac{r}{2R}\right) r^{D-1}\, \mathrm{d}r = \tfrac{1}{2}\kappa \frac{D-1}{\sqrt{2\pi}} \sum_{i=1}^N w_i \sigma_i' \tag{8}$$

where $S(D, r/2R)$ denotes the surface area of a zone on a sphere of radius 1. The zone is bounded by a virtual plane and the curved surface of the object. Both pass through the center of the sphere (cf. Fig. 1).

With $h = r/2R$, the function $S(D, h)$ is given by

$$S(D, h) = (DW(D, h) - hV(D-1)(1-h^2)^{(D-1)/2}) \tag{9}$$

where $W(D, h)$ is the volume of a sphere of radius 1 $(x_1^2 + x_2^2 + x_3^2 + \dots + t^2 \leqslant 1)$ that is enclosed between two planes, the lower at $t = 0$ and the upper at $t = h$, $h \leqslant 1$, (cf. Fig. 1b)

$$W(D, h) = \int_0^h V(D-1)(1-t^2)^{(D-1)/2}\, \mathrm{d}t\,. \tag{10}$$

In 2D, the zone length $S(2, r/2R)$ is

$$S(2, r/2R) = 2 \arcsin(r/2R) \tag{11}$$

and in 3D, the zone area $S(3, r/2R)$ is

$$S(3, r/2R) = 2\pi(r/2R) = \pi r \kappa\,. \tag{12}$$

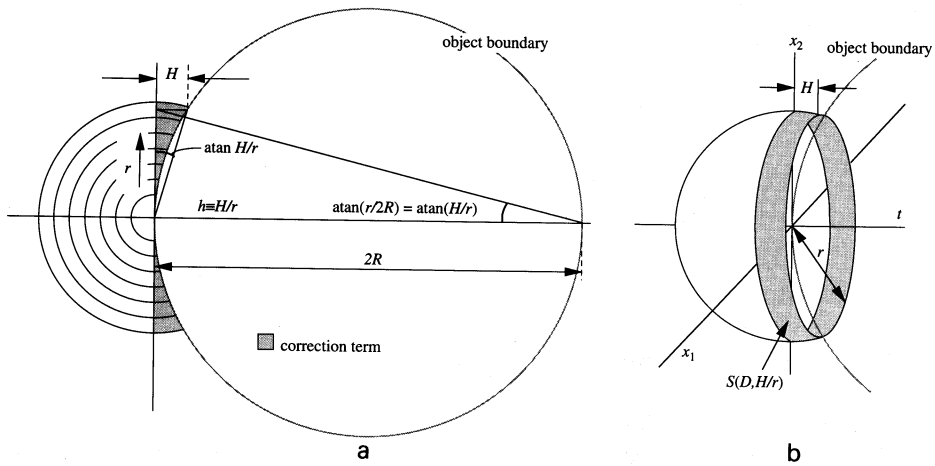

Fig. 1. Correction to the response of an isotropic filter due to edge curvature κ. (a) The hatched area outlines the difference in filter response between a constant-curvature edge and a straight edge. (b) The zone area on a sphere is bounded by a plane through x_1 and x_2 and the curved surface of the object.

For $D>3$, the zone areas $S(D, r/2R)$ are given by a recursive formula

$$S\left(D, \frac{r}{2R}\right) = \frac{2\pi}{(D-2)}\left(S\left(D-2, \frac{r}{2R}\right) + V(D-3)\,\frac{r}{2R}\left(1-\left(\frac{r}{2R}\right)^2\right)^{(D-3)/2}\right). \tag{13}$$

For $D>2$, κ must be read as the average curvature over the $(D-1)$-dimensional set of tangent directions; for $D=3$, $\kappa=\kappa_{\text{mean}}=\frac{1}{2}(\kappa_1+\kappa_2)$ with κ_1 and κ_2 being the principal curvatures.

Proof. The correction term equals the part of pillball volume that is bounded by a virtual plane on one side and the curve object surface on the other side. Because we calculate the correction term at the true edge position, both surfaces are passing through the pillball center. The hatched area in Fig. 1a shows the correction term in 2D. In order to derive the result given by Eq. (8) we start calculating the correction term for a single weighted Gaussian of size σ_i

$$\int_0^\infty w_i G_D(r, \sigma_i)\, S\left(D, \frac{r}{2R}\right) r^{D-1}\,\mathrm{d}r\,. \tag{14}$$

To find an expression for the area $S(D, r/2R)$ of a zone on a sphere, we start from an expression for the volume of a sphere ($x_1^2+x_2^2+x_3^2+\ldots+t^2\leqslant 1$ or $x_1^2+x_2^2+x_3^2\ldots\leqslant 1-t^2$) of radius 1

$$V(D) = \int_{-1}^{1} V(D-1)\,(1-t^2)^{(D-1)/2}\,\mathrm{d}t\,. \tag{15}$$

To obtain the volume $W(D, h)$ enclosed between 2 planes (the lower at $t=0$ and the upper at $t=h$, $h\leqslant 1$) we change the limits of integration accordingly

$$W(D, h) = \int_0^h V(D-1)\,(1-t^2)^{(D-1)/2}\,\mathrm{d}t\,. \tag{10}$$

For radius r and plane distance $rh=H$, the volume is $r^D W(D, H)$. The zone area $S(D, H/r)$ of a sphere of radius 1 is defined by

$$S(D,h)=S\left(D,\frac{H}{r}\right)=\frac{\partial}{\partial r}\left(r^D W\left(D,\frac{H}{r}\right)\right)\Big|_{r=1}=DW\left(D,\frac{H}{r}\right)-\frac{H}{r}V(D-1)\left(1-\left(\frac{H}{r}\right)^2\right)^{(D-1)/2} \tag{16}$$

with $h=H/r$. For $D=2$ and $D=3$, $S(D, r/2R)$ can easily be computed. The results are given in Eqs. (11) and (12). For $D>3$, the integral of Eq. (10) can be rewritten into a recursive formula using Spiegel(1968, eq. 14.396) after substitution of $a=1$ and $t=\sin(x)$. Together with Eq. (16) we obtain another recursive formula to compute $S(D, r/2R)$ for $D>3$

$$S\left(D,\frac{r}{2R}\right)=\frac{2\pi}{(D-2)}\left(S\left(D-2,\frac{r}{2R}\right)+V(D-3)h(1-h^2)^{(D-3)/2}\right). \tag{17}$$

Assuming small curvatures and therefore $h=r/2R\ll 1$ we can approximate $S(D, r/2R)$ by only taking the term with the lowest order in h

$$S(D,h)\approx V(D-1)(D-1)h=\tfrac{1}{2}(D-1)\kappa V(D-1)r. \tag{18}$$

Note that $S(D, h)$ is proportional to κ. The expression of $S(D, r/2R)$ is exact for $D=3$, but an approximation for $D\neq 3$. Substitution of Eq. (18) in Eq. (14) gives

$$w_i\tfrac{1}{2}\kappa V(D-1)\int_0^\infty G_D(r,\sigma_i)(D-1)r^D\,\mathrm{d}r=w_i\tfrac{1}{2}\kappa V(D-1)\int_0^\infty G_D(r,\sigma_i)\frac{D-1}{D+1}\,\mathrm{d}r^{D+1}$$

$$=w_i\tfrac{1}{2}\kappa\sqrt{2\pi\sigma_i^2}\,\frac{D-1}{D+1}V(D-1)\int_0^\infty G_{D+1}(r,\sigma_i)\,\mathrm{d}r^{D+1}.$$

Using Eq. (2), the integral can be eliminated. Now we have

$$=w_i\tfrac{1}{2}\kappa\sqrt{2\pi\sigma_i^2}\,\frac{D-1}{D+1}\,\frac{V(D-1)}{V(D+1)}$$

with $V(D)/V(D-2)=2\pi/D$ we get for the correction term for a single Gaussian

$$=w_i\tfrac{1}{2}\kappa\sigma_i\frac{D-1}{\sqrt{2\pi}}$$

which is due to $S(D, h)$ proportional to κ. The only natural length units are $R=\kappa^{-1}$ and σ_i. In order to make the correction term dimensionless, indeed only the product $\kappa\sigma_i$ can occur. Adding the results for N weighted Gaussians ($\{\sigma_i'\}$ instead of σ_i) we obtain the result of Eq. (8)

$$\int_0^\infty\left(\sum_{i=1}^N w_i G_D(r,\sigma_i')\right)S\left(D,\frac{r}{2R}\right)r^{D-1}\,\mathrm{d}r=\tfrac{1}{2}\kappa\frac{D-1}{\sqrt{2\pi}}\sum_{i=1}^N w_i\sigma_i'. \qquad \square$$

3.4. Filter requirements

We shall derive the weights $\{w_i\}$ and the conditions for which

1. the output of the MoG filter crosses zero at the position of the original step edge;
2. the weights of the MoG filter are independent of Gaussian pre-smoothing;
3. the weights of the MoG filter are independent of the edge curvature.

For a pseudo second-derivative filter we want zero response inside the object. Thus Eq. (6) should equal zero

$$\sum_{i=1}^N w_i=0. \tag{19}$$

This automatically guarantees a zero-crossing on a straight edge as Eq. (7) equals zero, $\frac{1}{2}\sum_{i=1}^{N} w_i = 0$.

A curvature-invariant zero-crossing requires that the correction term of Eq. (8) should equal zero

$$\sum_{i=1}^{N} w_i \sigma_i' = 0 . \tag{20}$$

For all $\sigma_i < \sigma_0$ we apply a Taylor series expansion to σ_i' (cf. Eq. (5)) around σ_0 and get

$$\sigma_i' = \sigma_0 \sqrt{1+\frac{\sigma_i^2}{\sigma_0^2}} \approx \sigma_0 \left(1 + \tfrac{1}{2}\frac{\sigma_i^2}{\sigma_0^2} - \tfrac{1}{8}\frac{\sigma_i^4}{\sigma_0^4} + \tfrac{1}{16}\frac{\sigma_i^6}{\sigma_0^6} - \tfrac{5}{128}\frac{\sigma_i^8}{\sigma_0^8} + O\left(\frac{\sigma_i^{10}}{\sigma_0^{10}}\right)\right).$$

Together with Eqs. (19) and (20) we get an infinite number of linear equations that are all independent of σ_0

$$\sum_{i=1}^{N} w_i \sigma_i^{2m} = 0, \quad m = 0, 1, 2, ..., \infty . \tag{21}$$

The number of equations that can be solved simultaneously (irrespective of the choice of $\{\sigma_i\}$) depends on the number of unknown variables $\{w_i\}$ in the equations. For a weighted sum of N Gaussians, $N-1$ equations ($0 \leqslant m \leqslant N-2$) can be satisfied. A single Gaussian ($N=1$) can never cause a zero-crossing. A single Gaussian with $w_1 > 0$ blurs the image an displaces the half-height position of all convex edges inwards.

3.5. Multiple-of-Gaussians (MoG)

The weights $\{w_i\}$ for N Gaussians can be found using linear algebra. The requirements of Eq. (21) can be seen as inner products between the vectors $\boldsymbol{w}$ and $\boldsymbol{\sigma}^{2m}$. The weight vector $\boldsymbol{w}$ should be perpendicular to the vectors $\boldsymbol{\sigma}^{2m}$ ($0 \leqslant m \leqslant N-2$). The multi-dimensional outer product of the $\boldsymbol{\sigma}^{2m}$ vectors fulfills this requirement

$$\boldsymbol{w} = \boldsymbol{\sigma}^0 \times \boldsymbol{\sigma}^2 \times ... \times \boldsymbol{\sigma}^{2(N-2)} = \begin{vmatrix} \boldsymbol{e}_1 & \boldsymbol{e}_2 & ... & \boldsymbol{e}_N \\ 1 & 1 & ... & 1 \\ \sigma_1^2 & \sigma_2^2 & ... & \sigma_N^2 \\ \vdots & \vdots & & \vdots \\ \sigma_1^{2(N-2)} & \sigma_2^{2(N-2)} & ... & \sigma_N^{2(N-2)} \end{vmatrix} \equiv |\Sigma| . \tag{22}$$

The individual weights w_i are given by the signed minors of $\boldsymbol{e}_i$ in Σ

$$\boldsymbol{w} = |\Sigma| = \sum_{j=1}^{N} (-1)^{1+j} |\Sigma_{1j}| \boldsymbol{e}_j \tag{23}$$

or (Vandermonde type determinant)

$$w_j = (-1)^{j+1} \prod_{\substack{k=1,...,N \\ k \neq j}} \prod_{\substack{l=1,...,N \\ l \neq j,k;\, l<k}} (\sigma_k^2 - \sigma_l^2) . \tag{24}$$

3.6. Doublet-of-Gaussians (DoG)

Two Gaussians are able to satisfy the first requirement (Eq. (21) for $m=0$). Any set of weights for which $w_1 = -w_2$ and $w_1 \neq 0$ may be used. Marr and Hildreth (1980) used DoG functions to model retinal center-surround receptive fields. Following the recipe of Eqs. (23) and (24) gives

$$w_1 = (-1)^{1+1} = 1, \qquad w_2 = (-1)^{2+1} = -1 . \tag{25}$$

3.7. Triplet-of-Gaussians (ToG)

Solving Eq. (21) for $m=0$ and $m=1$ gives the weights of the ToG filter

$$w_1=(-1)^{1+1}(\sigma_3^2-\sigma_2^2),\qquad w_2=(-1)^{2+1}(\sigma_3^2-\sigma_1^2),\qquad w_3=(-1)^{3+1}(\sigma_2^2-\sigma_1^2)\,. \tag{26}$$

The choice of the widths σ_1, σ_2, σ_3 is still free and will be studied experimentally in the next section.

4. Widths of Gaussians

In the previous section we have only required that $\sigma_i<\sigma_0$ (Taylor series expansion of σ_i'). The selection of $\{\sigma_i\}$ is a free choice. Without loss of generality we require that $\sigma_{i-1}<\sigma_i<\sigma_{i+1}$.

For example: $\sigma_1=1$ and $\sigma_N=2$. Now, we are still free to choose σ_i with $2\leqslant i\leqslant N-1$.

The above constraints lead to two interesting questions:

(1) How sensitive is the method for choices of $\sigma_i\approx\sigma_0$?

(2) Is the edge detection accuracy independent of the selection of σ_i with $2\leqslant i\leqslant N-1$?

A special case of point (2) is the limit of $\sigma_i\to\sigma_{i+1}$ (cf. Appendix A). Then a MoG filter changes into a weighted sum of one LoG filter and a series of MoG filters.

4.1. Selection of σ_2 for the ToG filter

The first two questions will be studied empirically for the ToG filter. We will set $\sigma_1=1$, $\sigma_3=2$ and vary σ_2 from 1.05 to 1.95 using increments of 0.05. Also the pre-smoothing σ_0 increases from 1 to $\frac{1}{2}R$. Fig. 2 shows the edge location error as obtained with our ToG filter. We notice that in 2D as well as in 3D the errors found are independent of σ_2. The errors of ToG increase with increasing pre-smoothing.

5. Error analysis

The relative error in zero-crossing position produced by MoG filtering can be estimated by dividing the MoG filter output at the true edge position by the slope of the filter output at that position. Applied to a spherical step-edge object of radius R, $u(R^2-r^2)$, we get

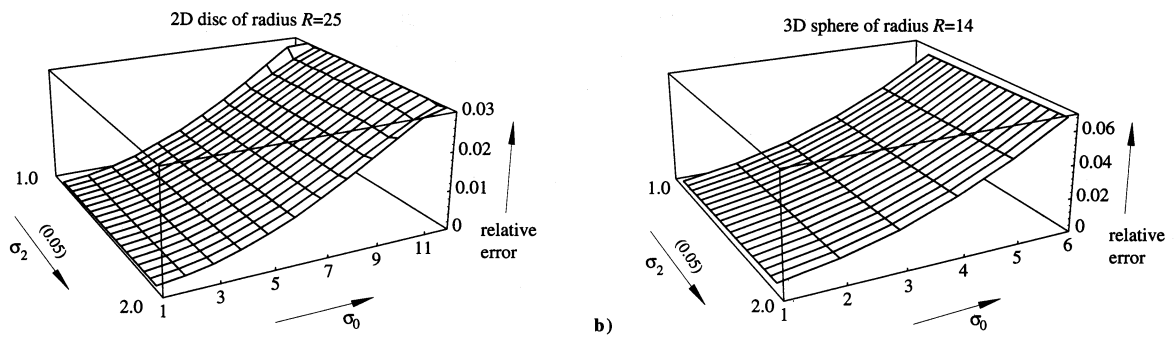

Fig. 2. Relative position error of a constant-curvature edge as a function of the size of pre-smoothing σ_0 and the size of σ_2 of the ToG filter. The smallest and largest Gaussians σ_1 and σ_3 were set respectively to 1.0 and 2.0. σ_2 varies from 1.05 to 1.95 using increments of 0.05. (a) A 2D disc of radius $R=25$ sampled at the Nyquist frequency. (b) A 3D sphere of radius $R=14$ sampled at the Nyquist frequency.

$$\frac{r_0-R}{R} \approx \frac{1}{R} \frac{\mathrm{MoG}(r, \{w_i\}, \{\sigma_i'\}, N)*u(R^2-r^2)}{\frac{\partial}{\partial r}\mathrm{MoG}(r, \{w_i\}, \{\sigma_i'\}, N)*u(R^2-r^2)}\Bigg|_{r=R}. \tag{27}$$

The numerator corresponds to the correction term of Eq. (8) using the weights of Section 3. The denominator can be calculated by adding the gradients produced by the N weighted Gaussians (cf. Appendix B).

Using Eqs. (8) and (27) and Appendix B we get for the relative location error of curved edges using a MoG filter

$$\frac{r_0-R}{R} \approx \frac{1}{R} \frac{(D-1)/(2R\sqrt{2\pi})\sum w_i\sigma_i'}{-1/\sqrt{2\pi}\sum w_i\sigma_i'^{-1}} = -\frac{(D-1)}{2R^2} \frac{\sum w_i\sigma_i'}{\sum w_i\sigma_i'^{-1}}. \tag{28}$$

To examine the errors of the MoG filters we apply a Taylor series expansion around $\sigma \equiv \sqrt{\sigma_0^2+\overline{\sigma_i^2}}$ to both the numerator and the denominator of Eq. (28) (cf. Table 1). The first non-zero terms in each expansion give the relative position error.

5.1. Comparison with second derivative operators

In earlier work we studied the location error of three second-derivative filters when applied to curved edges (2D and 3D) after low-pass filtering (Verbeek and van Vliet, 1993; van Vliet, 1993). These filters are: the Laplacian ($B_{xx}+B_{yy}+B_{zz}$), the second derivative in the gradient direction (SDGD=B_{gg}, with g the gradient direction) and their sum (PLUS=Laplace+SDGD). All derivative operators are implemented as a convolution with a derivative of a Gaussian (Canny, 1986). Table 2 summarizes the results for Gaussian low-pass filtered curved edges in 2D and 3D images. Examination of Table 2 reveals that MoG filters with more than two Gaussians exhibit a smaller error than Laplace and SDGD.

6. Experiments

To test this theory we will perform some experiments. The test objects are simulated images of a bandlimited disc or sphere sampled at the Nyquist rate.

6.1. Implementation

The MoG filter with or without an additional digital pre-smoother can be effectively implemented in the Fourier domain. After an FFT, the spectrum is multiplied by the corresponding Gaussian transfer functions and

Table 1
Taylor series expansion around $\sigma \equiv \sqrt{\sigma_0^2+\overline{\sigma_i^2}}$ of the numerator (MoG correction term, $\propto \Sigma w_i\sigma_i'$) and the denominator (gradient MoG, $\propto \Sigma w_i\sigma_i'^{-1}$). The leading terms determine the relative location error for N Gaussians. The quotient $1/(2N-3)$ of leading terms shows the reduction of the relative location error with increasing N.

Position of first non-zero term	$N=2$ ↓	$N=3$ ↓	$N=4$ ↓	$N=5$ ↓
$\sum w_i\sigma_i'$	$\approx\sigma_0\Big(\sum w_i$	$+\frac{1}{2}\sum w_i\frac{\sigma_i^2}{\sigma_0^2}$	$-\frac{1}{8}\sum w_i\frac{\sigma_i^4}{\sigma_0^4}$	$+\frac{1}{16}\sum w_i\frac{\sigma_i^6}{\sigma_0^6}$ $-\frac{5}{128}\sum w_i\frac{\sigma_i^8}{\sigma_0^8}+\ldots\Big)$
$\sum w_i\sigma_i'^{-1}$	$\approx\sigma_0^{-1}\Big(\sum w_i$	$-\frac{1}{2}\sum w_i\frac{\sigma_i^2}{\sigma_0^2}$	$+\frac{3}{8}\sum w_i\frac{\sigma_i^4}{\sigma_0^4}$	$-\frac{5}{16}\sum w_i\frac{\sigma_i^6}{\sigma_0^6}$ $+\frac{7\times5}{128}\sum w_i\frac{\sigma_i^8}{\sigma_0^8}-\ldots\Big)$
Quotient of leading terms	$-\frac{1}{1}$	$-\frac{1}{3}$	$-\frac{1}{5}$	$-\frac{1}{7}$

Table 2
Relative location error of constant curvature edges as function of the total σ ($\sigma^2=\sigma^2_{\text{slope}}+\sigma^2_{\text{PSF}}+\sigma^2_{\text{smooth}}+\overline{\sigma_i^2}\equiv\sigma_0^2+\overline{\sigma_i^2}$) and the radius of osculating circle (sphere) at every edge location. The positive axis is defined from the center of the object. For all second-derivative filters (Verbeek and van Vliet, 1993; van Vliet, 1993) and all MoG filters with $N\geqslant 2$ we describe the relative radial displacement of the (middle) zero-crossing.

Filter	$D=2$	$D=3$	D	*Edge criterion*
MoG_1	$\approx -\frac{1}{2}\left(\frac{\sigma}{R}\right)^2$	$\approx -\left(\frac{\sigma}{R}\right)^2$	$\approx -\frac{1}{2}(D-1)\left(\frac{\sigma}{R}\right)^2$	half height
MoG_2	$\approx \frac{1}{2}\left(\frac{\sigma}{R}\right)^2$	$\approx \left(\frac{\sigma}{R}\right)^2$	$\approx \frac{1}{2}(D-1)\left(\frac{\sigma}{R}\right)^2$	zero-crossing
MoG_N	$\approx \frac{1}{2N-3}\frac{1}{2}\left(\frac{\sigma}{R}\right)^2$	$\approx \frac{1}{2N-3}\frac{1}{2}\left(\frac{\sigma}{R}\right)^2$	$\approx \frac{1}{2N-3}\frac{1}{2}(D-1)\left(\frac{\sigma}{R}\right)^2$	zero-crossing
LoG	$(0.45\pm 30\%)\left(\frac{\sigma}{R}\right)^2$	$(0.83\pm 20\%)\left(\frac{\sigma}{R}\right)^2$	$\approx \frac{1}{2}(D-1)\left(\frac{\sigma}{R}\right)^2$	zero-crossing
SDGD	$-(0.29 \text{ to } 1.3)\left(\frac{\sigma}{R}\right)^2$	$-(0.5 \text{ to } 4.0)\left(\frac{\sigma}{R}\right)^2$	$\approx -\frac{1}{2}(D-1)\left(\frac{\sigma}{R}\right)^2$	zero-crossing
PLUS	$(0.43\pm 14\%)\left(\frac{\sigma}{R}\right)^4$	$(1.1\pm 10\%)\left(\frac{\sigma}{R}\right)^4$	$\approx \frac{1}{2}(D-1)\left(\frac{\sigma}{R}\right)^4$	zero-crossing

scaled using the proper weight factors. The sum of the filtered and scaled spectra can be transformed back using an inverse FFT.

Gaussian filters can also effectively be implemented in the spatial domain. The D-dimensional filter can be decomposed into D one-dimensional filters along the coordinate axes of the image. A Gaussian FIR filter is created by sampling the Gaussian function and truncate it at a few times σ. However, this truncation (even at five times σ) causes unpredictable behavior of the MoG filters. Implementation in the Fourier domain is simple and not affected by this problem.

6.2. Prediction versus experiment

Fig. 3 shows the prediction as well as the measured relative position error (relative bias (r_0-R/R) of MoG filters up to five Gaussians. We notice an excellent correspondence between the theory and the measured errors for a 3D sphere. In 2D, the MoG_5 filter shows a discrepancy between theory and practice for relatively large values of the pre-smoothing. The error bars are smaller than the plot symbols and therefore omitted.

6.3. Robustness in the presence of noise

When the signal-to-noise ratio decreases, the coefficient-of-variation (CV) will increase and eventually the bias will increase. For noise-free images, the CV's are an order of magnitude smaller than the reported bias.

We have investigated the robustness of the 3D MoG filters applied to a sphere of radius 10. The sphere was sampled at the Nyquist rate and the maximum digital smoothing was set to a Gaussian filter with $\sigma_{\text{smooth}}=4$. In 2D we repeated the experiment with a disc of radius 25 sampled at the Nyquist rate. Here the maximum digital smoothing was set to 10. Each SNR requires a minimum amount of smoothing to allow accurate prediction of the edge shift (Table 3). An accurate prediction can take place when the measurement error is small compared to predicted bias. The experiments were performed using a MoG_4 filter. The MoG_4 filter was chosen because it is the filter with the smallest edge shift that performs exactly as predicted (see previous section).

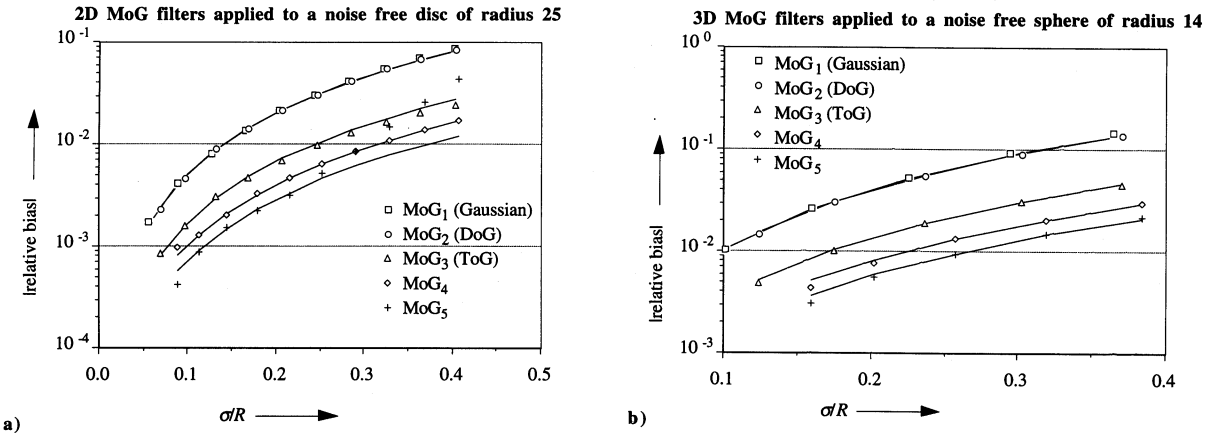

Fig. 3. Relative location error (relative bias) of MoG filters. The MoG filter is composed of fixed σ_i's (spaced by a factor $\alpha\sigma^2_{\mathrm{MoG}}$ around σ^2_{MoG}) and a variable pre-smoothing σ_0. The relative bias is plotted as function of the relative filter size (σ/R) with $\sigma^2=\sigma_0^2+\sigma^2_{\mathrm{MoG}}$. (a) The MoG filters are applied to a disc of radius 25 sampled at the Nyquist rate. For DoG and ToG $\sigma^2_{\mathrm{MoG}}=2$ and $\alpha=0.5$. For MoG_4 and MoG_5 $\sigma^2_{\mathrm{MoG}}=4$ and $\alpha=3/8$. (b) The MoG filters are applied to a sphere of radius 14 sampled at the Nyquist rate.

Table 3
Minimum amounts of digital smoothing that allows accurate prediction of the resulting edge shift given a SNR. The experiments were performed using a MoG_4 filter.

SNR		2D, $R=25$ Gaussian smoothing σ_{smooth}	3D, $R=10$ Gaussian smoothing σ_{smooth}
100	40 dB	≥ 0	≥ 0
50	34 dB	≥ 1.5	≥ 1
20	26 dB	≥ 2.5	≥ 1
10	20 dB	≥ 5	≥ 2
5	14 dB	≥ 8	≥ 3
2	6 dB	≥ 10	≥ 4

7. Conclusions

This paper describes the systematic displacement of curved edges due to filtering with a linear combination of Gaussians. A single Gaussian displaces the half-height position of a convex curved edge inwards. The shift is $-\frac{1}{2}(D-1)(\sigma/R)^2$. Using two Gaussians we construct a DoG filter with a zero-crossing at the estimated edge position. For convex edges, the DoG zero-crossing lies outside the object $+\frac{1}{2}(D-1)(\sigma/R)^2$.

MoG filters with more than two Gaussians produce multiple zero-crossings. The central and "strongest" one is selected for edge localization. The central zero-crossing is displaced with respect to the true object boundary. The edge shift is a constant fraction of the one produced by the DoG filter. The fractions for three, four and five Gaussians are: 1/3, 1/5, and 1/7. For N Gaussians the edge shift is $1/(2N-3)$ times the one produced by a DoG filter (or LoG).

Practical values for widths of the Gaussians are spaced by a factor $\alpha\sigma^2_{\mathrm{MoG}}$ around σ^2_{MoG}. For DoG and ToG $\sigma^2_{\mathrm{MoG}}=2$ and $\alpha=0.5$. For MoG_4 and MoG_5 $\sigma^2_{\mathrm{MoG}}=4$ and $\alpha=3/8$:

- Dog: $\{\sigma_i^2\}=\{1, 3\}$,
- ToG: $\{\sigma_i^2\}=\{1, 2, 3\}$,
- MoG_4: $\{\sigma_i^2\}=\{1, 2.5, 5.5, 7\}$,
- MoG_5: $\{\sigma_i^2\}=\{1, 2.5, 4, 5.5, 7\}$.

Experiments (cf. Table 3) have shown that a decreasing SNR requires a larger digital smoothing filter (σ_0) to produce a sufficiently smooth contour (2D) or surface (3D) and to allow accurate prediction of the resulting edge shift. We have restricted ourselves to edge radii a few times (2 to 3) larger than the total Gaussian smoothing. Situations around corners as studied by Berzins (1984) for instance for Laplace filtering cannot be described using the presented theory.

8. Appendix A: The limit of $\sigma_{N-1} \to \sigma_N$

DoG. Set $\sigma_1^2 = \sigma^2$ and $\sigma_2^2 = \sigma^2 + \varepsilon$. With $w_1 = 1$ and $w_2 = 1$ and $\varepsilon \to 0$ the DoG filter becomes

$$\mathrm{DoG}(\{\sigma_1, \sigma_2\}, r)_{\varepsilon \to 0} = G_D(\sigma, r) - G_D(\sqrt{\sigma^2 + \varepsilon}, r) \approx -\varepsilon \frac{\partial}{\partial(\sigma^2)} G_D(\sigma, r) = -\frac{\varepsilon}{2} \mathrm{LoG}(\sigma, r)$$

with $\mathrm{LoG}(\sigma, r)$ the Laplacian-of-Gaussian. The DoG filter changes into a LoG filter.

ToG. Set $\sigma_1^2 = \sigma^2 - \Delta$, $\sigma_2^2 = \sigma^2$, and $\sigma_3^2 = \sigma^2 + \varepsilon$ with $\varepsilon \ll \Delta$. With $w_1 = \varepsilon$, $w_2 = -(\varepsilon + \Delta)$, $w_3 = \Delta$ and $\varepsilon \to 0$ the ToG filter becomes

$$\begin{aligned}\mathrm{ToG}(\{\sigma_i\}, r)_{\varepsilon \to 0} &= \varepsilon(G_D(\sigma_1, r) - G_D(\sigma_2, r)) + \Delta(G_D(\sqrt{\sigma^2 + \varepsilon}, r) - G_D(\sigma, r)) \\ &\approx \varepsilon\, \mathrm{DoG}(\{\sigma_1, \sigma_2\}, r) + \Delta\varepsilon \frac{\partial}{\partial(\sigma^2)} G_D(\sigma, r) \\ &= \varepsilon\left(\mathrm{DoG}(\{\sigma_1, \sigma_2\}, r) + \frac{\Delta}{2} \mathrm{LoG}(\sigma, r)\right).\end{aligned}$$

Note that the gradients of DoG and LoG have opposite signs, i.e., the central part of a DoG is positive whereas the central part of a LoG is negative. The ToG filter changes into a weighted sum of DoG and LoG.

MoG. Set $\sigma_N^2 = \sigma^2 + \varepsilon$ and $\sigma_i^2 = \sigma^2 - (N - i + 1)\Delta$ for $1 \leqslant i \leqslant N$ with $\varepsilon \ll \Delta$. If $\varepsilon \to 0$ the MoG filter becomes

$$\mathrm{MoG}(r, \{\sigma_i\}, N)_{\varepsilon \to 0} \approx \varepsilon \alpha_1 \Delta^N \mathrm{LoG}(r, \sigma) + \varepsilon \sum_{n=2}^{N-1} \alpha_n \frac{\Delta^{N-1}}{\Delta^{(n-2)(n-1)/2}} \mathrm{MoG}(r, \{\sigma_{N-n}, \ldots, \sigma_{N-1}\}, n).$$

In general, a MoG filter changes into a weighted sum of one LoG filter and a series of MoG filters (with fewer Gaussians than the MoG filter we started with).

9. Appendix B: Gradient of a Gaussian filtered constant-curvature step edge in two and three dimensions

The gradient at the true edge position of a curved edge (B_g at $r = R$) after filtering with a single Gaussian of size σ is calculated as follows:

$$B_g = \frac{V(D-1)}{2^{D-1}} \int_0^{l_{\max}} h_l c^{D-1}(l)\, \mathrm{d}l \tag{29}$$

with B the Gaussian filtered images, h_l the derivative of the filter shape and $c(l)$ the chord diameter of the intersection between an object of radius R and a pillball filter of radius l positioned at the true edge radius $r = R$. For a D-dimensional Gaussian filter h_l is

$$h_l = \frac{\partial}{\partial l} \frac{\mathrm{e}^{-l^2/2\sigma^2}}{(2\pi\sigma^2)^{D/2}} = -l \frac{\mathrm{e}^{-l^2/2\sigma^2}}{\sigma^2 (2\pi\sigma^2)^{D/2}}. \tag{30}$$

For all D, the pillball at the true edge position, c^2 is given by

$$c^2(l)=4l^2-l^4/R^2\,. \tag{31}$$

For $l \ll R$, c can be approximated by

$$c(l)=2l\sqrt{1-l^2/4R^2}\approx 2l(1-l^2/8R^2)\,. \tag{32}$$

Substitution of Eqs. (30) and (32) in Eq. (29) gives

$$B_g=-\frac{V(D-1)}{(2\pi)^{D/2}}\int_0^{l_{\max}}\frac{e^{-l^2/2\sigma^2}}{\sigma^{D+2}}\,l^D(1-l^2/8R^2)^{D-1}\,dl\,. \tag{33}$$

For $D=2$, with $\xi=l/\sigma$ and $\sigma \ll R$

$$B_g=-\frac{1}{\pi}\left(\int_0^{l_{\max}}\frac{e^{-\xi^2/2}}{\sigma}\,\xi^2\,d\xi-\sigma\int_0^{l_{\max}}\frac{e^{-\xi^2/2}}{8R^2}\,\xi^4\,d\xi\right)=-\frac{1}{\pi}\left(\frac{I(2,\infty)}{\sigma}-\frac{\sigma I(4,\infty)}{8R^2}\right)\approx-\frac{1}{\sqrt{2\pi}\,\sigma}\,, \tag{34}$$

for $D=3$, with $\xi=l/\sigma$ and $\sigma \ll R$

$$B_g=-\frac{1}{2\sqrt{2\pi}}\left(\int_0^{l_{\max}}\frac{e^{-\xi^2/2}}{\sigma}\,\xi^3\,d\xi-\sigma\int_0^{l_{\max}}\frac{e^{-\xi^2/2}}{4R^2}\,\xi^5\,d\xi\right)=-\frac{1}{2\sqrt{2\pi}}\left(\frac{I(3,\infty)}{\sigma}-\frac{\sigma I(5,\infty)}{4R^2}\right)\approx-\frac{1}{\sqrt{2\pi}\,\sigma} \tag{35}$$

with $I(n, \infty)$ the nth moment of a Gaussian filter. In first-order approximation the gradient of a Gaussian filtered constant-curvature step edge is independent of the curvature.

10. References

Berzins, V. (1984). Accuracy of Laplacian edge detectors. *Computer Vision, Graphics, and Image Processing* 27, 195–210.

Canny, J. (1986). *A computational approach to edge detection. IEEE Trans. Pattern Anal. Machine Intell.* 8 (6), 679–698.

Koenderink, J.J. (1984). The structure of images, *Biol. Cybernet.* 50, 363–370.

Marr, D. and E.C. Hildreth (1980). Theory of edge detection. *Proc. Roy. Soc. London* B 207, 187–217.

Spiegel, M.R. (1968). *Schaum's Outline Series: Mathematical Handbook of Formulas and Tables.* MacGraw-Hill, New York.

van Vliet, L.J. (1993). Grey-Scale Measurements in Multi-Dimensional Digitized Images. Ph. D. Thesis, Delft University Press, Stevinweg 1, 2628 CN Delft, The Netherlands.

van Vliet, L.J., I.T. Young, and A.L.D. Beckers (1989). A nonlinear Laplace operator as edge detector in noisy images. *Computer Vision, Graphics, and Image Processing* 45 (2), 167–195.

Verbeek, P.W., and L.J. van Vliet (1993). On the location error of curved edges in low-pass filtered 2D and 3D images. *IEEE Trans. Pattern Anal. Machine Intell.*, in press.

Witkin, A. (1983). Scale-space filtering. *Internat. Joint Conf. on Artificial Intelligence*, Karlsruhe, Germany, 1019–1021.